Preparation and Photocatalytic Activity of Zinc Sulfide/Polymer Nanocomposites

Zhengfa Zhou, Yan Feng, Weibing Xu, Fengmei Ren, Haihong Ma

Department of Polymer Science and Engineering, Hefei University of Technology, Hefei 230009, China

Received 11 May 2008; accepted 16 January 2009
DOI 10.1002/app.30139
Published online 2 April 2009 in Wiley InterScience (www.interscience.wiley.com).

ABSTRACT: ZnS nanoparticles were prepared on the surface of polyacrylonitrile (PAN) and methyl methacrylate (MMA)/butyl methacrylate (BMA)/acrylic acid (AA) copolymer nanofibers. The MMA–BMA–AA copolymer was synthesized by bulk radical polymerization using 2,2′-azobisisobutyronitrile as the initiator. The PAN and MMA–BMA–AA copolymer nanofibers were prepared by electrospinning. Zinc ions were introduced onto the surface of the nanofibers by coordination with the carboxyl of AA. Then, sulfide ions were added to react with zinc ions to form ZnS nanoparticles. The average diameter of the nanofibers was about 300 nm, and the diameter of the ZnS nanoparticles was about 10 nm. The band position of the photoluminescence spectrum of the ZnS/PAN and MMA–BMA–AA nanocomposites had an 80-nm blueshift in comparison with that of the corresponding bulk ZnS sample. The ZnS/PAN and MMA–BMA–AA nanocomposites had high photocatalytic activity for the degradation of phenol under ultraviolet irradiation; the photocatalytic activity changed indistinctively after it was used repeatedly (6 times). The nanofibers of PAN and MMA–BMA–AA not only dispersed but also stabilized the ZnS nanoparticles. © 2009 Wiley Periodicals, Inc. J Appl Polym Sci 113: 1264–1269, 2009

Key words: catalysts; fibers; nanocomposites

INTRODUCTION

Metal sulfides, such as ZnS and CdS, are well-known semiconductors that have been used in the photocatalytic degradation of toxic organic compounds in water and air.[1–3] The dispersion and stability of metal sulfides used as photocatalysts are still big challenges for researchers. Attempts have been made to improve the dispersion of metal sulfide by, for example, the use of inorganic materials as supports and the preparation of metal sulfides on a nanoscale.[4–8]

Inorganic/organic hybrid materials with unique properties derived from the combinatorial effects of organic and inorganic phases have attracted much attention in recent years.[9,10] Gou et al.[11] used poly (vinyl chloride), $ZnCl_2$, and Na_2S to prepare a conjugated polymer/ZnS complex. They found that the conjugated polymer/ZnS complex could extend the absorption band to the visible region, had extremely high photocatalytic activity for the degradation of dyes, and played an important role in the photocatalytic degradation. Dai et al.[12] prepared the coordination polymer $[(ZnS)_2(en)]_\infty$ by a solvothermal method from elemental sulfur and zinc(II) salt in ethylenediamine. They found that the compound had comparatively good photocatalytic activity for the degradation of dyestuff X-2R. Polymeric materials may improve the dispersion and stability of metal sulfides by affecting the surface area, bandgap, morphology, and surface defects of metal sulfides.[13]

In this article, we present a novel and simple approach for hybridizing ZnS nanoparticles and polymer-based nanofibers via the electrospinning technique and the coordination effect. This process involves five steps: (1) synthesizing the methyl methacrylate (MMA)/butyl methacrylate (BMA)/acrylic acid (AA) copolymer, (2) preparing a sol with suitable polyacrylonitrile (PAN) and MMA–BMA–AA copolymer content for electrospinning, (3) electrospinning the solution to obtain nonwoven polymer nanofibers, (4) introducing zinc ions to coordinate with carboxyls of the nanofibers, and (5) introducing sulfide ions to form ZnS nanocrystals on the surface of the polymer nanofibers.

For these as-synthesized hybrid nanocomposites, the quantization effects, catalytic properties of ZnS nanoparticles, and easy processability of polymer nanofibers are integrated, and they can be manipulated easily and reclaimed conveniently as photocatalysts.

Correspondence to: Z. Zhou (zhengfazhou@sohu.com).
Contract grant sponsor: National Natural Science Foundation of China; contract grant number: 20776034.
Contract grant sponsor: Doctoral Fund of Ministry of Education of China; contract grant number: 20070359036.

EXPERIMENTAL

Materials and characterization

PAN obtained from Anqing Petrochemical Corp. (Anging, China) was dried at 65°C for 5 h before use. The other chemicals were purchased from Shanghai Chemicals (Shanghai, China) and used without further purification. The morphologies of the products were observed with a JSM 6700F field-emission scanning electron microscope (JEOL Ltd., Tokyo, Japan) and a JEOL 2010 high-resolution transmission electron microscope (JEOL Ltd., Tokyo, Japan). Selected area electron diffraction was also recorded on the JEOL 2010 high-resolution transmission electron microscope. The chemical composition of the products was characterized with X-ray photoemission spectroscopy (XPS; MK-II, Escalab) (VG Scientific Ltd., East Grinstead, UK). The photoluminescence results were obtained with a Fluorolog 3-Tau spectrophotometer (Horiba Jobin Yuon, Longjumeau Cedex, France).

Preparation of the MMA–BMA–AA copolymer

MMA (30 g), 40 g of BMA, 30 g of AA, and 0.5 g of 2,2′-azobisisobutyronitrile were added to a 250-mL, three-necked flask equipped with a condenser, a stirrer, and an N_2 inlet. After polymerizing at 80°C for 40 min, the reaction mixture was transferred to a stainless steel plate and placed in an oven at 40°C for 12 h. Then, the reaction mixture was maintained at 100°C for 3 h to polymerize the remainder of the monomer, and the MMA–BMA–AA copolymer was obtained.

Electrospinning

PAN (12 g) or 10.3 g of PAN and 1.7 g of the MMA–BMA–AA copolymer were dissolved in 88 g of *N*,*N*-dimethylformamide. The solution was electrospun at a positive voltage of 30 kV, at a working distance of 25 cm (the distance between the needle tip and the target), and at a flow rate of 2.0 mL/h. All manipulations were carried out at room temperature.

Preparation of the ZnS/polymer nanocomposites

The electrospinning mats were immersed into a $ZnCl_2$ aqueous solution of the desired concentration in a flask for 24 h. The carboxyl on the surface of the electrospinning nanofibers was coordinated with a cluster of Zn^{2+} ions. Afterwards, the mats were removed from the solution and washed with distilled water three times. Then, the mats were immersed into an $(NH_2)_2CS$ aqueous solution of the desired concentration, the pH of the solution was adjusted to 9 with an aqueous solution of NaOH, and the immersion time was kept at 1 h at 70°C under the protection of N_2. The sulfide resource was introduced by this processing, and ZnS nuclei formed and grew into nanoparticles under the drive of the combining force between Zn^{2+} ions and S^{2-} ions. Subsequently, the mats were removed and washed with distilled water three times, and the ZnS/polymer nanocomposites were obtained.

Photocatalytic activity

The photocatalytic activity of ZnS/PAN and MMA–BMA–AA nanocomposites under ultraviolet (UV) irradiation was measured by the decomposition rate of phenol in an aqueous solution. The experiments were processed on a UV photocatalytic apparatus (XPA-2, Nanjing Xujiang Machine Co., Nanjing, China). A 300-W halogen lamp with wavelengths of 360–380 nm was positioned inside a cylindrical Pyrex vessel, which was surrounded by a circulating water jacket to cool the lamp. ZnS/PAN and MMA–BMA–AA nanocomposites (0.0558 g) were suspended in a 500-mL, 40.6 mg/L phenol aqueous solution. During the degradation, 10 mL of the phenol aqueous solution was extracted every 30 min and titrated with a 0.0242 mol/L Na_2SO_3 aqueous solution.

RESULTS AND DISCUSSION

Morphology of the ZnS/polymer nanocomposites

Figure 1(a) shows a representative scanning electron microscopy (SEM) image of the PAN and MMA–BMA–AA copolymer nanofibers (the weight ratio of PAN to the MMA–BMA–AA copolymer was 6 : 1) produced by electrospinning. The products consisted of a large quantity of randomly deposited fiberlike morphologies. According to the measurements, the average diameter of the PAN and MMA–BMA–AA copolymer nanofibers was about 300 nm. Figure 1(b) shows the morphology of the PAN and MMA–BMA–AA copolymer nanofibers compounded with ZnS nanoparticles, which are described as ZnS/PAN and MMA–BMA–AA nanocomposites in this article. There were some particles, whose average diameter was less than 100 nm, along the nanofibers, in contrast to the smooth surface of the nanofibers in Figure 1(a), whereas there were large agglomerated particles, which did not disperse well, along the pure PAN nanofibers [Fig. 1(c)]. It can be speculated that the existence of carboxyl groups of the MMA–BMA–AA copolymer provided more nucleation centers for ZnS and prevented the assembly of particles. Therefore, the PAN and MMA–BMA–AA copolymer nanofibers were used in the following experiments.

Figure 2 shows ZnS particles that grew in $ZnCl_2$ and $(NH_2)_2CS$ solutions of different concentrations. The quantity of ZnS particles increased with the concentration of the $ZnCl_2$ and $(NH_2)_2CS$ solution increasing.

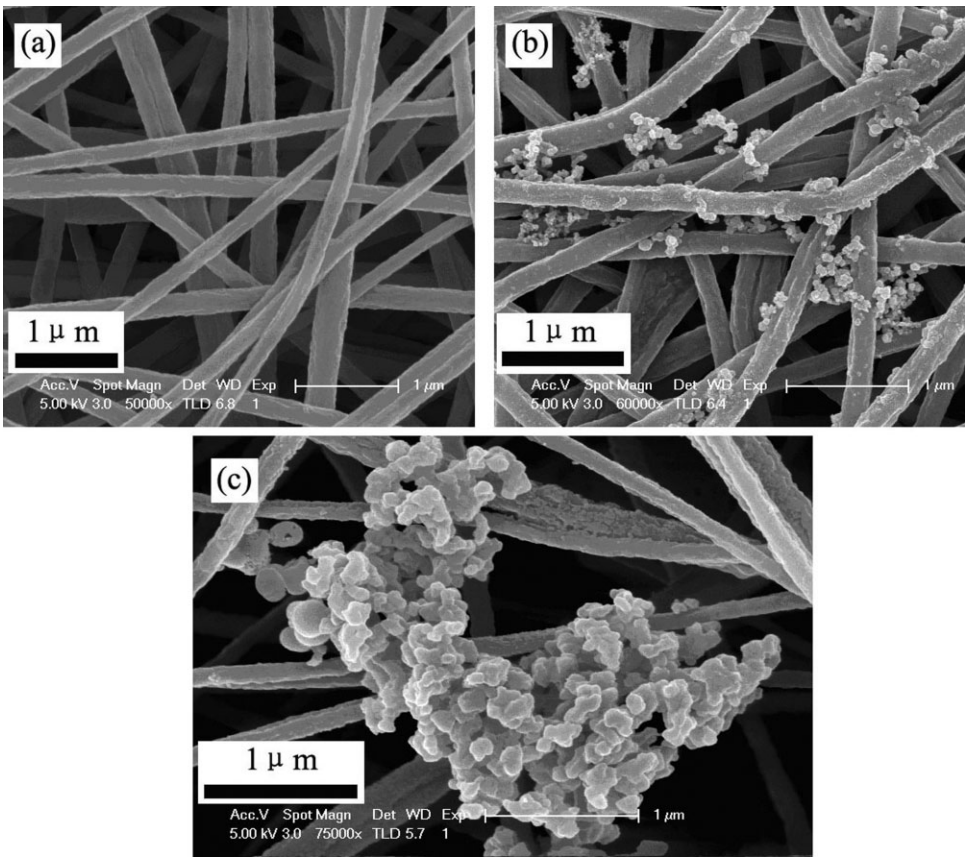

Figure 1 SEM images of (a) nanofibers of the PAN and MMA–BMA–AA copolymer produced by electrospinning, (b) ZnS/PAN and MMA–BMA–AA nanocomposites, and (c) ZnS/PAN nanocomposites [0.05 mol/L $ZnCl_2$ and 0.05 mol/L $(NH_2)_2CS$ were used for parts b and c].

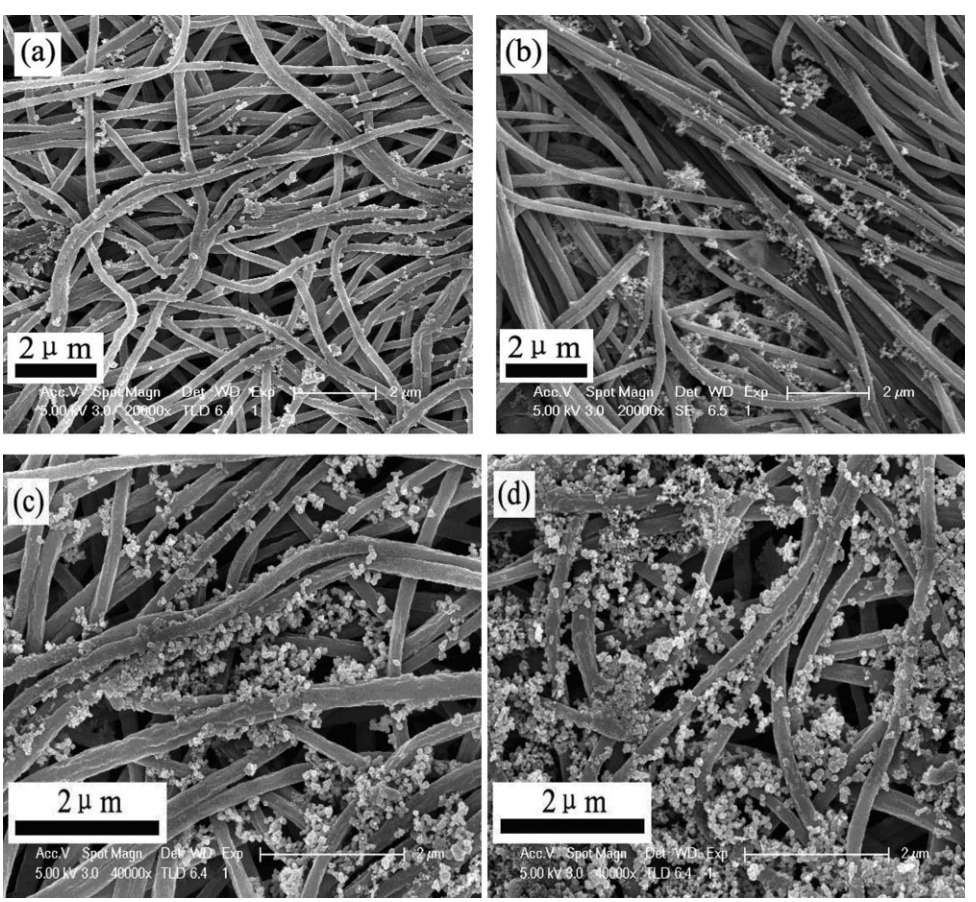

Figure 2 SEM images of ZnS/PAN and MMA–BMA–AA nanocomposites: (a) 0.02 mol/L $ZnCl_2$ and 0.02 mol/L $(NH_2)_2CS$, (b) 0.1 mol/L $ZnCl_2$ and 0.1 mol/L $(NH_2)_2CS$, (c) 0.2 mol/L $ZnCl_2$ and 0.2 mol/L $(NH_2)_2CS$, and (d) 0.5 mol/L $ZnCl_2$ and 0.5 mol/L $(NH_2)_2CS$.

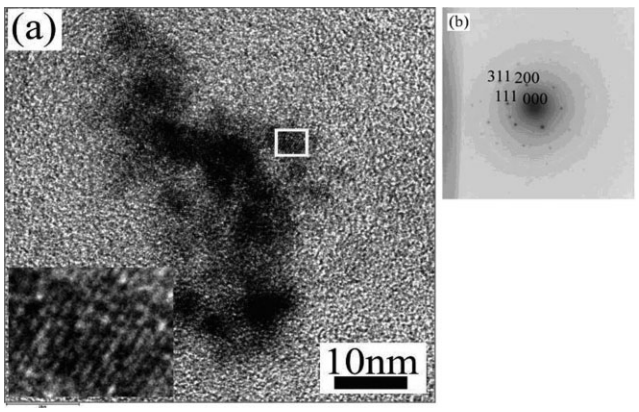

Figure 3 (a) HRTEM image of ZnS/PAN and MMA–BMA–AA nanocomposites and (b) a selected area diffraction pattern of the sample.

Characterization of the ZnS/polymer nanocomposites

Figure 3 shows high-resolution transmission electron microscopy (HRTEM) images of ZnS/PAN and MMA–BMA–AA nanocomposites. Figure 3(a) reveals that the particles, which are shown in Figure 1(b), were composed of many nanoparticles. The corresponding high-magnification image [inset of Fig. 3(a)] shows that the average diameter of the nanoparticles was about 10 nm with a lattice constant of 0.42 nm. The selected area electron diffraction pattern [Fig. 3(b)] clearly shows the diffraction spots of ZnS instead of diffraction rings of polycrystalline ZnS, and this indicates that the selected area of the ZnS nanocrystals had a single crystalline structure. It also reveals that these microcrystalline structures were composed of cubic ZnS (JCPDS no. 80-0020). It can be speculated that the existence of the polymer passivated the surface activity of the particles and prevented the assembly of particles.

The composition of the ZnS/PAN and MMA–BMA–AA nanocomposites was examined by XPS, which is shown in Figure 4; both the survey spectra [Fig. 4(a)] and zinc LMM (The Auger effect of zinc element) [Fig. 4(b)] are displayed. From the survey spectra, we can find that the product consisted of carbon, oxygen, nitrogen, zinc, and sulfur chemistry elements, which corresponded to the PAN, MMA–BMA–AA copolymer, and ZnS, and the binding energy values were 1022.34 eV for $Zn2p_3$ and 161.73 eV for S2p, respectively. The kinetic energy for zinc LMM was 988.60 eV.

These results are consistent with the values of ZnS nanocrystals.[14] The quantification of peaks gave a ratio of zinc to sulfur of 1.37 : 1, and this meant that the number of zinc atoms was larger than that of sulfur atoms. The reaction mechanism of Zn^{2+} ions with S^{2-} ions can be conjectured as follows. At first, the carboxyl was coordinated with Zn^{2+} ions. After the sulfide resource was introduced, ZnS nuclei formed and grew into nanoparticles under the drive of the combining force between Zn^{2+} ions and S^{2-} ions. However, there were still some Zn^{2+} ions coordinated with carboxyl. That is why the number of zinc atoms was larger than that of sulfur atoms.

Figure 5 shows photoluminescence excitation (PLE) and photoluminescence emission (PL) spectra of ZnS/PAN and MMA–BMA–AA nanocomposites. The PLE peak observed at 268 nm is in good agreement with the band edge estimated from the absorption spectra. The PL spectrum illustrated in Figure 5(b) shows a broad blue emission with a peak position at 389 nm assigned to the electron–hole recombination from internal vacancies for zinc and sulfur atoms. There is a prominent blueshift of about 80 nm of the emission band in comparison with that of the bulk ZnS,[15] and this may be due to the quantum size effects of the ZnS nanoparticles.

Photocatalytic activity

The UV irradiation photocatalytic activity of ZnS/PAN and MMA–BMA–AA nanocomposites was

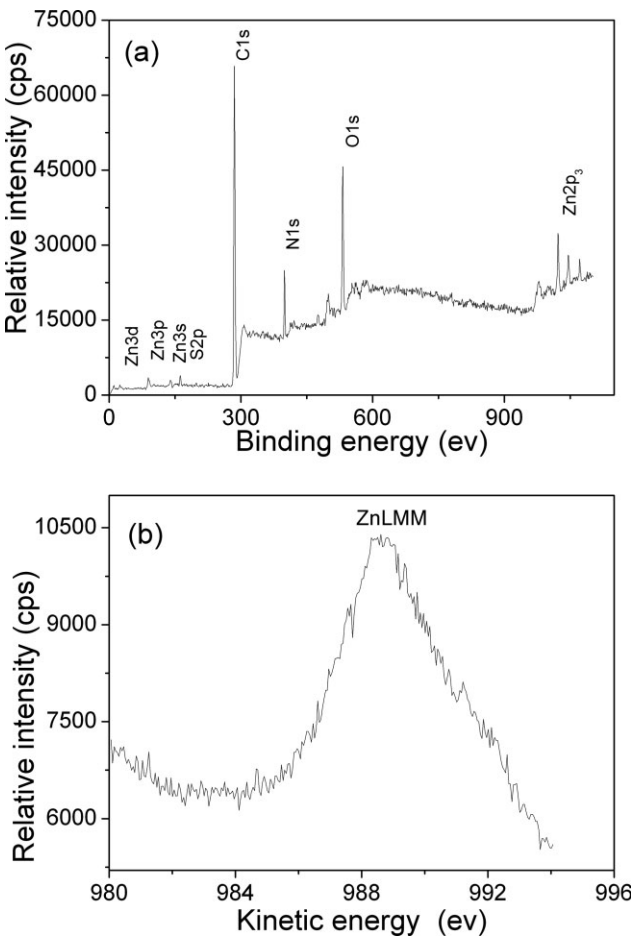

Figure 4 XPS spectra of ZnS/PAN and MMA–BMA–AA nanocomposites: (a) survey spectrum and (b) zinc LMM.

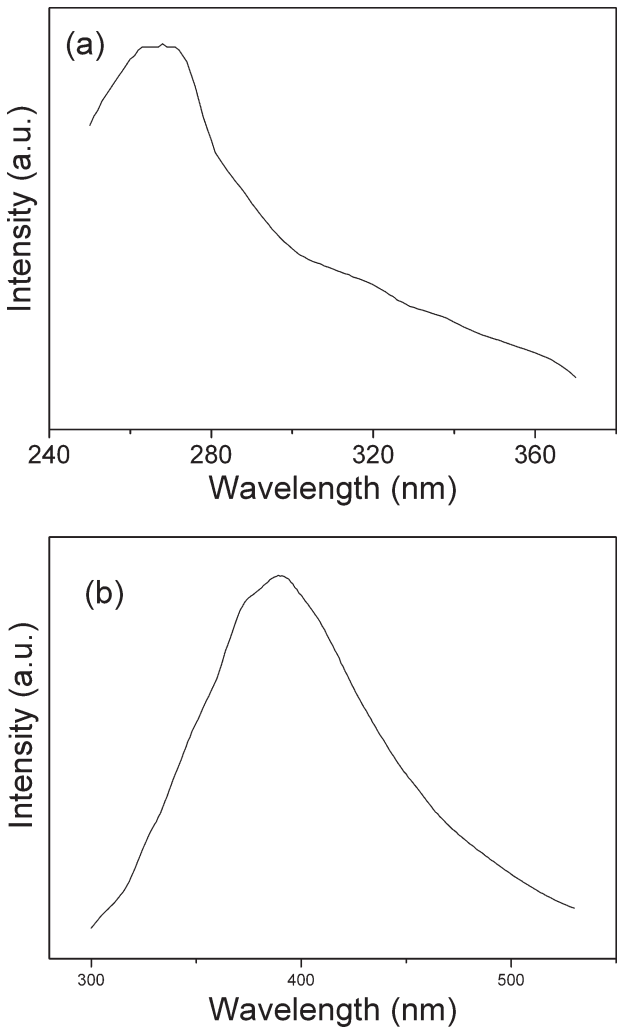

Figure 5 (a) PLE and (b) PL spectra of ZnS/PAN and MMA–BMA–AA nanocomposites.

investigated through the degradation of a 500-mL, 40.6 mg/L (C_0) phenol aqueous solution. The results for 2 h of irradiation are shown in Figure 6. The phenol aqueous solution was degraded 91.3% [calculated by $(C_0 - C)/C_0$] (C is the concentration of phenol agueous solution during degradation) under UV irradiation catalyzed with ZnS/PAN and MMA–BMA–AA nanocomposites for 2 h, whereas the sample without the catalyst (used for comparison) was degraded 6.93%. The weight of the ZnS/PAN and MMA–BMA–AA nanocomposites used in this experiment was 0.0558 g, but the weight of ZnS in the nanocomposites was 0.0011 g; this was obtained by calcination of the nanocomposites in an SRJX (Shenyang, China) 8-13 high-temperature box resistance oven at 600°C for 6 h. The concentration of ZnS was about 2.2 mg/L; this result shows that the ZnS/PAN and MMA–BMA–AA nanocomposites had higher photocatalytic activity in comparison with earlier reports.[12,16] The ZnS/PAN and MMA–BMA–AA nanocomposites were used repeatedly (6 times)

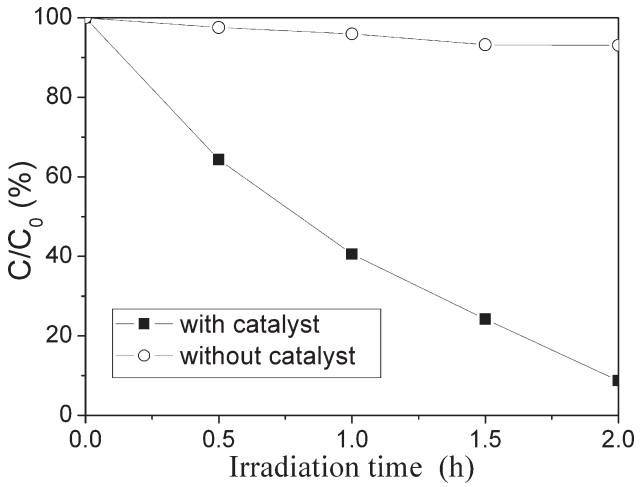

Figure 6 Photocatalytic degradation of phenol aqueous solutions under UV.

as catalysts to degrade the phenol aqueous solution. The results are shown in Figure 7. It reveals that the photocatalytic activity of the ZnS/PAN and MMA–BMA–AA nanocomposites changed indistinctively. This may be due to the fact that the nanofibers of PAN and MMA–BMA–AA not only dispersed but also stabilized the ZnS nanoparticles.

CONCLUSIONS

In summary, we have presented a novel route for fabricating ZnS nanoparticles on the surface of PAN and MMA–BMA–AA copolymer nanofibers. The band position of the photoluminescence spectrum of the ZnS/PAN and MMA–BMA–AA nanofibers had an 80-nm blueshift in comparison with that of the corresponding bulk ZnS sample. The polymer nanofibers enhanced the quantum effects of the ZnS

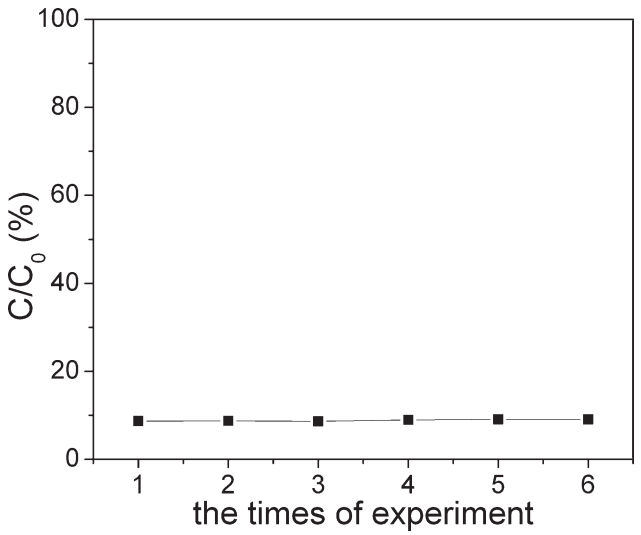

Figure 7 Effect of the repeat times on the photocatalytic activity of ZnS/PAN and MMA–BMA–AA nanocomposites.

nanoparticles. The ZnS/PAN and MMA–BMA–AA nanocomposites had high photocatalytic activity for the degradation of phenol under UV irradiation; the photocatalytic activity changed indistinctively after being used repeatedly (6 times). The nanofibers of PAN and MMA–BMA–AA not only dispersed but also stabilized the ZnS nanoparticles.

References

1. Torres-Martinez, C. L.; Kho, R.; Mian, O. I.; Mehra, R. K. J Colloid Interface Sci 2001, 240, 525.
2. Kim, C.; Doh, S. J.; Lee, S. G.; Lee, S. J.; Kim, H. Y. Appl Catal A 2007, 330, 127.
3. Fu, H. B.; Pan, C. S.; Yao, W. Q.; Zhu, Y. F. J Phys Chem B 2005, 109, 22432.
4. Guan, G.; Kida, T.; Kusakabe, K.; Kimura, K.; Abe, E.; Yoshida, A. Appl Catal A 2005, 295, 71.
5. Shangguan, W. F.; Yoshida, A. J Phys Chem B 2002, 106, 12227.
6. Anil, K.; Anshuman, J. J Colloid Interface Sci 2006, 297, 607.
7. Ghosh, P. K.; Ahmed, S. F.; Jana, S.; Chattopadhyay, K. K. Opt Mater 2007, 29, 1584.
8. Chang, M.; Cao, X. L.; Xu, X. J.; Zhang, L. Phys Lett A 2007, 10, 1016.
9. Forster, S.; Antonietti, M. Adv Mater 1998, 10, 195.
10. Ni, Y.; Zheng, S. X.; Nie, K. M. Polymer 2004, 45, 5557.
11. Gou, Y. Q.; Su, Z. X.; Xue, Z. Q. Mater Res Bull 2004, 39, 2203.
12. Dai, J.; Jiang, Z. J.; Li, W. G.; Bian, G. Q.; Zhu, Q. Y. Mater Lett 2002, 55, 383.
13. Chen, J. B.; Lin, S.; Yan, G. Y.; Yang, L. Y.; Chen, X. Q. Catal Commun 2008, 9, 65.
14. Zhang, Y. C.; Wang, G. Y.; Hu, X. Y.; Shi, Q. F.; Qiao, T.; Yang, Y. J Cryst Growth 2005, 284, 554.
15. Yang, P.; Lü, M. K.; Meng, F. Q.; Song, C. F.; Xu, D. Opt Mater 2004, 27, 103.
16. Shao, H. F.; Qian, X. F.; Zhu, Z. K. J Solid State Chem 2005, 178, 3522.